MicroRNA-155-5p inhibits trophoblast cell proliferation and invasion by disrupting centrosomal function

YUNG-CHIEH TSAI[1,2*], TIAN-NI KUO[1*], RUEI-CI LIN[3], HUI-LING TSAI[4], YU-YING CHAO[3], PEI-RONG LEE[3], PING-JUI SU[5] and CHIA-YIH WANG[3,4]

[1]Department of Obstetrics and Gynecology, Chi-Mei Medical Center, Tainan 710; [2]Department of Sport Management, Chia Nan University of Pharmacy and Science, Tainan 717; [3]Institute of Basic Medical Sciences; [4]Department of Cell Biology and Anatomy, College of Medicine, National Cheng Kung University, Tainan 701; [5]Division of General Surgery, Department of Surgery, National Cheng Kung University Hospital, Tainan 704, Taiwan, R.O.C.

Received November 15, 2023; Accepted February 22, 2024

DOI: 10.3892/mmr.2024.13209

Abstract. Recurrent miscarriage is used to refer to more than three pregnancy failures before 20 weeks of gestation. Defective trophoblast cell growth and invasion are frequently observed in recurrent miscarriage. Several microRNAs (miRs), including miR-155-5p, are aberrantly upregulated in recurrent miscarriage; however, the underlying molecular mechanisms remain unclear. The centrosome orchestrates microtubule networks and coordinates cell cycle progression. In addition, it is a base for primary cilia, which are antenna-like organelles that coordinate signaling during development and growth. Thus, deficiencies in centrosomal functions can lead to several disease, such as breast cancer and microcephaly. In the present study, the signaling cascades were analyzed by western blotting, and the centrosome and primary cilia were observed and analyzed by immunofluorescence staining. The results showed that overexpression of miR-155-5p induced centrosome amplification and blocked primary cilia formation in trophoblast cells. Notably, centrosome amplification inhibited trophoblast cell growth by upregulating apoptotic cleaved-caspase 3 and cleaved-poly (ADP-ribose) polymerase in miR-155-5p-overexpressing trophoblast cells. In addition, overexpression of miR-155-5p inhibited primary cilia formation, thereby inhibiting epithelial-mesenchymal transition and trophoblast cell invasion. All phenotypes could be rescued when cells were co-transfected with the miR-155-5p inhibitor, thus supporting the role of miR-155-5p in centrosomal functions. It was also found that miR-155-5p activated autophagy, whereas disruption of autophagy via the depletion of autophagy-related 16-like 1 alleviated miR-155-5p-induced apoptosis and restored trophoblast cell invasion. In conclusion, the present study indicated a novel role of miR-55-5p in mediating centrosomal function in recurrent miscarriage.

Correspondence to: Dr Ping-Jui Su, Division of General Surgery, Department of Surgery, National Cheng Kung University Hospital, 138 Sheng Li Road, Tainan 704, Taiwan, R.O.C.
E-mail: cookieray1210@hotmail.com

Professor Chia-Yih Wang, Department of Cell Biology and Anatomy, College of Medicine, National Cheng Kung University, 1 University Road, Tainan 701, Taiwan, R.O.C.
E-mail: b89609046@gmail.com

*Contributed equally

Abbreviations: ARL13B, ADP-ribosylation factor-like 13B; ATG16L1, autophagy-related 16-like 1; CEP164, centrosomal protein 164; EMT, epithelial-mesenchymal transition; ERK, extracellular signal-regulated kinase; IGFBP1, insulin-like growth factor binding protein-1; IFT88, intraflagellar transport 88; MPA, medroxyprogesterone 17-acetate; SOX9, sex-determining region Y-box 9; T-HESC, telomerase-immortalized human endometrial stromal cell; THBS1, thrombospondin 1

Key words: microRNA-155-5p, trophoblast, invasion, cell growth, centrosome, primary cilia

Introduction

Recurrent miscarriage is used to refer to more than three pregnancy failures before 20 weeks of gestation. Recurrent miscarriage affects 1-2% of couples globally and ~50% of cases have no identifiable cause worldwide (1). The incidence of recurrent miscarriage is ~1/300 pregnancies (2). Recurrent miscarriage is a complex pathological condition that can be caused by gestational infection, defective hormone homeostasis, genetic defects, poor endometrial differentiation or other unexplained factors (3). Placenta formation is an essential step for a successful pregnancy; it involves a well-orchestrated interplay between the blastocyst and the receptive endometrium (4,5). Thus, defective placentation can lead to complications, such as preeclampsia or recurrent implantation failure (6,7).

Uterine endometrial differentiation and trophoblast invasion are crucial for early placenta formation. During implantation, the trophectoderm of the blastocyst invades the maternal uterine wall followed by the generation of cytotrophoblasts (8). These trophoblast cells undergo epithelial-mesenchymal transition (EMT) and invade the maternal uterine stroma layer (9). The migration and invasion

of trophoblasts mediate the formation of the placenta and the remodeling of the maternal spiral arterial walls. Thus, defective trophoblast proliferation and invasion cause several complications, including preeclampsia and recurrent miscarriage (9).

MicroRNAs (miRNAs/miRs) are non-coding RNAs comprised of 20-24 nucleotides that post-transcriptionally mediate gene translation (10). Through binding to the 3'-untranslated region, miRNAs mediate mRNA translation or stability. Hairpin pre-miRNAs are exported from the nucleus to the cytoplasm where they are processed by the ribonuclease Dicer (11). Mature miRNAs then bind to the RNA-induced silencing complex to mediate mRNA stability (12). Dysregulation of miRNAs has been widely studied in several diseases, and in neuronal development and cancer progression. For example, miR-450a is a tumor suppressor that inhibits ovarian cancer cell growth, EMT and metastasis (13). In addition, miR-195 facilitates *de novo* lipogenesis to inhibit breast cancer cell migration and invasion (14). Moreover, miRNAs mediate female reproduction (15,16). Overexpression of miR-30-5p has been reported to induce ferroptosis of trophoblasts, thus causing preeclampsia (17). Furthermore, miR-141 and miR-200a inhibit the expression of endocrine gland-derived vascular endothelial growth factor, thus preventing preeclampsia (18). Furthermore, aberrant expression of miRNA signatures, including miR-20b-5p, miR-155-5p and miR-718, is associated with recurrent miscarriage (19). Despite miRNAs being involved in early pregnancy, the underlying molecular mechanism remains unclear.

The centrosome is composed of a pair of centrioles, mother and daughter centrioles, and the outer protein matrix pericentriolar materials. The centrosome, the primary microtubule-organizing center of cells, maintains cell shape, and directional migration or segregation of duplicated chromosomes into daughter cells equally during the M phase (20,21). In addition to regulating microtubule dynamics, the centrosome functions as a center to coordinate cell cycle progression (22). Cyclin E localizes to the centrosome to promote G1/S transition (23). Disruption of centrosome integrity by depleting centrosomal proteins arrests the cells in the G0/G1 phase (24). Thus, precise control of centrosome function and homeostasis maintains cell cycle progression.

During the quiescent stage or under stress, the primary cilia grow from the mother centriole of the centrosome. The primary cilia are composed of the basal body (mother centriole), microtubule-based axoneme and the outer ciliary membranes (24,25). Unlike motile cilia, primary cilia are immotile antenna-like structures that conduct extracellular signaling during development (26). Several signaling receptors, such as receptor tyrosine kinase, G protein-coupled receptors or hedgehog signaling, reside on the ciliary membrane to coordinate environmental cues (27,28). Dysfunction of primary cilia causes many disorders during development and differentiation, which are collectively termed ciliopathies (26). Primary cilia also play important roles in successful pregnancy. Primary cilia are observed in the placenta during the first trimester of pregnancy. These primary cilia activate extracellular signal-regulated kinase (ERK) signaling to promote placenta formation (29,30). Thus, defective primary cilia formation leads to preeclampsia and other complications such as gestational diabetes mellitus (30).

Previous studies have shown that miR-155-5p is dysregulated in recurrent miscarriage; however, the underlying molecular mechanism remains unclear (19,31). The present study, we will investigate whether miR-155-5p inhibits trophoblast cell growth and invasion. MiR-155-5p mimic or inhibitor will be transfected into trophoblast cells followed by examining cell migration and invasion. In addition, to uncover the underlying molecular mechanism, the centrosome homeostasis and primary ciliogenesis were also examined. Thus, the data will uncover the role of miR-155-5p in mediating centrosomal functions and trophoblast cell growth and invasion.

Materials and methods

Cell culture and drug treatment. The human immortalized endometrial stroma telomerase-immortalized human endometrial stromal cells (T-HESCs) and HTR-8/SVneo (HTR8) trophoblast cells were maintained in RPMI-1640 medium (Gibco; Thermo Fisher Scientific, Inc.) supplemented with 10% fetal bovine serum (Gibco; Thermo Fisher Scientific, Inc.), 1% glutamine, 1% sodium pyruvate and 1% penicillin/streptomycin under a humidified atmosphere containing 5% CO_2 at 37˚C. The HTR8 cell line was established using extravillous cytotrophoblasts freshly isolated from a first-trimester placenta and transfected with a plasmid containing the simian virus 40 large T antigen (32). This cell line contains two populations, one of epithelial and one of mesenchymal origin (33). For triggering decidualization *in vitro*, T-HESCs were treated with 0.3 mM 8-Bromo-cAMP (cat. no. BML-CN115; Enzo Life Sciences) and 10 μM medroxyprogesterone 17-acetate (MPA) at 37˚C for 72 h. To block centrosome amplification, cells were treated with 250 nM Centrinone (LCR-263, cat. no. HY-18682; MedChemExpress) at 37˚C for 72 h. To activate p38, cells were treated with 1 μM sodium salicylate (cat. no. S3007; MilliporeSigma) at 37˚C for 72 h.

miRNA and small interfering RNA (siRNA) transfection. A commercially available siRNA against autophagy-related 16-like 1 (ATG16L1; SMARTpool; GE Healthcare Dharmacon, Inc.), and miRNA mimics or inhibitors (miRIDIAN microRNA; GE Healthcare Dharmacon, Inc.) were purchased from Horizon Discovery. The siRNA and miRNA sequences were as follows: SMARTpool-siATG16L1 (5'-UGUGGAUGAUUAUCGAUUA-3'; 5'-GGCACACACUCACGGGACA-3'; 5'-GCAUUGGAUUAACGGAAAC-3'; 5'-GUUAUUGAUCUCCGAACAA-3'); miR-20b-5p mimic (5'-CAAAGUGCUCAUAGUGCAGGUAG-3'); miR-155-5p mimic (5'-UUAAUGCUAAUCGUGAUAGGGGU-3'); miR-718 inhibitor (5'-CUUCCGCCCCGCCGGGCGUCG-3'); and miR-155-5p inhibitor (5'-UUAAUGCUAAUCGUGAUAGGGGU-3'). The negative controls of miRNA mimics and inhibitors were commercially available. The miRNA mimic negative control (5'-UCACAACCUCCUAGAAAGAGUAGA-3'; cat. no. MIMAT0000039) was purchased from Horizon Discovery (GE Healthcare Dharmacon, Inc.). miRNA inhibitor negative control (5'-UUGUACUACACAAAAGUACUG-3'; cat. no. MIMAT0000295) was purchased from Horizon Discovery (GE Healthcare Dharmacon, Inc.). The scrambled siRNA with the target sequence 5'-GAUCAUACGUGCGAUCAGA-3' was purchased from Sigma (MilliporeSigma).

Cells were transfected with 50 nM miRNA or siRNA using Lipofectamine 2000 (Invitrogen; Thermo Fisher Scientific, Inc.) at 37˚C for 72 h. Samples were collected and analyzed immediately. To investigate the role of p38 in modulating primary cilia, SB203580 (working concentration, 10 μM; Abcam) was used to inhibit the function of p38 at 37˚C for 72 h.

Western blotting. Cells were trypsinized and lysed with CelLytic™ MT cell lysis reagent (MilliporeSigma) containing protease inhibitor for 10 min on ice. Lysates were centrifuged at 13,000 x g for 10 min at 4˚C and the supernatant was collected. The protein concentration was determined using the Bio-Rad protein quantity assay (Bio-Rad Laboratories, Inc.) by BioSpectrometer® (Eppendorf AG, Germany). The samples (50 μg/lane) were mixed with 2X sample buffer and heated to 100˚C for 10 min. Equal amounts of proteins were separated by 10% sodium dodecyl sulfate-polyacrylamide gel electrophoresis at 150 V for 90 min. Following gel separation, the samples were transferred to PVDF membranes at 20 V overnight. Next, the membrane was blocked with 3% BSA (MilliporeSigma) dissolved in TBST (0.005% Tween) at room temperature for 1 h and incubated with the following antibodies: Anti-Akt (cat. no. #4691; Cell Signaling Technology, Inc.), anti-phospho-Akt (Thr308; cat. no. #9275; Cell Signaling Technology, Inc.), anti-ATG16L1 (cat. no. #8089S; Cell Signaling Technology, Inc.), anti-cleaved-caspase 3 (cat. no. #9664; Cell Signaling Technology, Inc.), anti-cleaved-poly (ADP-ribose) polymerase (PARP; cat. no. #9542; Cell Signaling Technology, Inc.), anti-cyclin A (cat. no. ab38; Abcam), anti-cyclin D (cat. no. 2G3G5; Thermo Fisher Scientific, Inc.), anti-cyclin E (cat. no. #4132; Cell Signaling Technology, Inc.), anti-1A/1B light chain 3B (LC3A/B; cat. no. #12741; Cell Signaling Technology, Inc.), anti-matrix metalloproteinase 2 (MMP2; cat. no. #40994; Cell Signaling Technology, Inc.), anti-p38 (cat. no. #9212; Cell Signaling Technology, Inc.), anti-phospho-p38 (cat. no. 09-272; Merck KgaA), anti-p44/42 mitogen-activated protein kinase (ERK1/2; cat. no. #4695; Cell Signaling Technology, Inc.), anti-phospho-ERK1/2 (cat. no. #4370; Cell Signaling Technology, Inc.) and anti-actin (cat. no. ab8227; Abcam) in 1:10,000 dilutions at 4˚C overnight. After washing with TBST for 30 min, the membrane was incubated with an HRP-conjugated secondary antibody (ab205718, Abcam) in 1:7,000 at room temperature for 1 h. Subsequently, the signals were detected by the ECL kit (MilliporeSigma) with actin as the loading control and analyzed by ImageJ (version 1.53k, National Institutes of Health, USA).

Immunofluorescence microscopy. Cells were fixed and permeabilized in ice-cold pure methanol (MilliporeSigma) for 5 min at -20 ˚C. After permeabilization, cells were incubated in blocking buffer [containing 0.2% Triton X-100, 0.05% Tween-20 and normal goat serum (MilliporeSigma)] for 1 h at room temperature and incubated with the following antibodies: Anti-acetylated tubulin (cat. no. T6793; MilliporeSigma), anti-ADP-ribosylation factor-like 13B (ARL13B; cat. no. 17711-1-AP; Proteintech Group, Inc.), anti-centrosomal protein 164 (CEP164; cat. no. NBP1-81445; Novus Biologicals, LLC), anti-intraflagellar transport 88 (IFT88; cat. no.13967-1-AP; Proteintech Group, Inc.) and anti-γ-tubulin (cat. no. T6557; MilliporeSigma) in 1:700 dilutions at 4˚C for overnight. After which, the cells were washed for 30 min with PBS three times and were then incubated with FITC- or Cy3-conjugated goat anti-mouse or anti-rabbit IgG secondary antibodies (cat. nos. ab175473 and ab150077; Abcam) in 1:700 dilutions in the presence of 6-diamino-2-phenylindole at room temperature for 1 h at room temperature. The cells were then further washed for 30 min with PBS three times. The coverslips were overlaid on 50% glycerol in PBS and the signals were observed through an Axio imager D2 fluorescence microscope and analyzed by ZEN 2 blue edition software (Zeiss AG).

Reverse transcription-quantitative (RT-q)PCR. Total RNA was extracted using TRI reagent (MilliporeSigma) and Direct-zol™ RNA miniprep (Zymo Research Corp.). RNA (1 μg) was then reverse transcribed into cDNA using an RT kit (sensiFAST; Bioline) according to manufacturer's protocol. Fast SYBR Green Master Mix (MilliporeSigma) was used to perform qPCR with a final concentration of 0.25 nM gene-specific primers. The sequences of the primers were as follows: E-cadherin forward: 5'-CCGAGAGCTACACGTTC-3', reverse: 5'-TCTTCAAAATTCACTCTGCC-3'; fibronectin-1 forward: 5'-CCATAGCTGAGAAGTGTTTTG-3', reverse 5'-CAAGTACAATCTACCATCATCC-3'; MMP2 forward: 5'-GTGATCTTGACCAGAATACC-3', reverse: 5'-GCCAATGATCCTGTATGTG-3'; thrombospondin 1 (THBS1) forward: 5'-GTGACTGAAGAGAACAAAGAC-3', reverse 5'-CAGCTATCAACAGTCCATTC-3'; and zinc-finger E-box-binding homeobox 1 (ZEB-1) forward: 5'-AAAGATGATGAATGCGAGTC-3', reverse: 5'-TCCATTTTCATCATGACCAC-3'. PCR signals were compared among groups after normalization, with GAPDH forward: 5'-TCGGAGTCAACGGATTTG-3', reverse: 5'-CAACAATATCCACTTTACCAGAG-3') used as the internal reference, calculated using the $2^{-\Delta\Delta Cq}$ method (18,34,35). The thermocycling conditions were as follows: 95 ˚C for 10 min. Next, they were denatured at 95˚C for 15 sec and annealing the primer with DNA template at 60˚C for 1 min. These cycles were repeated for 40 times.

Wound healing assay. HTR8 cells were plated on 6-well plates and transfected with miR-155-5p mimic and/or inhibitor prior to the migration assay. A wound was created by scratching the cells with a sterile 200-μl pipette tip, and fresh medium (serum-free) was added to the cells after washing with PBS. The microscopy images of the cells migrating into the wound area were captured at x10 magnification under an optical microscope at 0 and 12 h after scraping, in order to record the wound closure area. Wound closure was calculated using the following formula: Wound closure (%)=100-(initial area of wound-nth h area of the wound)/(initial area of the wound).

Cell invasion assay. The cell invasion assay was performed using Falcon cell culture inserts (pore size, 8 μm) according to the manufacturer's protocol. Matrigel (1 mg/ml at 37˚C; Corning, Inc.) was loaded onto the upper chambers of the inserts for 30 min, whereas the lower chamber contained a serum-loaded medium as an attractant. Cells were seeded and overlaid on the Matrigel at a density of $3x10^4$ cells/well in serum-free medium. Upon termination of the incubation at 37˚C for 24 h, invasive cells were fixed in 100% methanol for

4 min and stained with Giemsa's azure eosin methylene blue solution (Merck KGaA) at room temperature for 2 h at room temperature and cell numbers were counted in six high-power fields per insert under an optical microscope. The experiments were performed in triplicate and repeated three times.

Cell growth assay. HTR8 cells were plated at a density of $1x10^5$ cells on a 6-well plate. After incubating cells for 24, 48 and 72 h, cells were trypsinized and resuspended with 1 ml PBS for cell counting with hemocytometer. All treatments were carried out in triplicate, with each experiment performed three times.

EdU assay. HTR8 cells were seeded on 25x25-mm coverslips in 6-well tissue culture plates and transfected with the miR-155-5p mimic and/or inhibitor. The cell proliferation ability was measured using Click-iT® EdU Imaging Kits (Thermo Fisher Scientific, Inc.). Briefly, 1 μl 10 μM EdU working solution (Component A) was added and incubated at 37˚C for 1 h. After which, the cells were permeabilized in ice-cold methanol for 5 min. Subsequently, 1X Click-iT® EdU buffer was added, as per the manufacturer's instructions, and incubated at 37˚C for 1 h. The cells were then washed for 30 min with PBS three times and the signals were observed under an Axio imager D2 fluorescence microscopy (Zeiss AG).

ELISA. Supernatants from different experimental groups were analyzed using insulin-like growth factor binding protein-1 (IGFBP1; cat. no. ab233618, Abcam) and prolactin (cat. no. ab226901; Abcam) ELISA kits according to the manufacturer's instructions. Briefly, supernatants were added to each well followed by addition of 50 μl antibody cocktails and shaking at 30 x g at 37˚C for 1 h. Then, each well was washed with 350 μl PBS three times. After washing, 50 μl TMB development solution was added to each well, followed by the termination of the reaction via the addition of a stop solution. The solution was measured at 450 nm.

Bioinformatics. The predicted target gene of miR-20b-5p was conducted by 2.0 of the miRNA Pathway Dictionary Database (miRPathDB), which was freely accessible at https://mpd.bioinf.uni-sb.de/. MiRPathDB 2.0 performed analysis of the underlying metabolic pathway and potential miRNA targets, and with customized application, generated the relation chart of predicted centrosome-associated target genes of miR-20b-5p.

Statistical analysis. Values from the experimental assays are expressed as the mean ± SEM of ≥3 independent experimental repeats. Differences between two groups or >2 groups were compared using unpaired Student's t-test or one-way ANOVA with Dunnett's post hoc test, respectively. Data were analyzed using GraphPad Prism version no.9 (Dotmatics). $P<0.05$ was considered to indicate a statistically significant difference. All experiments are repeated at least for three times.

Results

miR-20b-5p, miR-155-5p or miR-718 inhibitor do not affect decidualization. Aberrant expression levels of miR-20b-5p, miR-155-5p and miR-718 have been observed in women who suffer from recurrent miscarriage (19). To investigate the underlying molecular mechanisms, uterine endometrial differentiation, and trophoblast growth and invasion, which are essential events for successful pregnancy, were examined. It was first checked whether aberrant expression levels of these miRNAs affected endometrial stromal cell growth. Overexpression of miR-20b-5p and miR-155-5p were used to mimic the upregulation of these two miRNAs, and transfection with a miR-718 inhibitor was used to induce downregulation of miR-718 in T-HESCs. T-HESCs were transfected with miR-20b-5p, miR-155-5p and miR-718 inhibitor (Fig. 1A-C), and cell numbers were counted. Transfection with all three miRNAs had no effects on T-HESC growth (Fig. 1D), suggesting that miR-20b-5p, miR-155-5p and miR-718 inhibitor did not affect endometrial stromal cell growth. After which, the ability of uterine endometrial stromal differentiation, known as decidualization, was examined. Decidualization was induced by treating T-HESCs with cAMP and MPA for 3 days, followed by examining the decidual markers IGFBP1 and prolactin. Prolactin and IGFBP1 levels were significantly increased upon cAMP and MPA co-treatment (Fig. 1E and F). After which, the effects of miR-20b-5p, miR-155-5p and miR-718 inhibitor on decidualization were examined. Transfection of cells with miR-20b-5p, miR-155-5p or miR-718 inhibitor did not affect the levels of prolactin and IGFBP1 (Fig. 1G and H), suggesting that these miRNAs did not disturb endometrial decidualization.

Overexpression of miR-155-5p inhibits trophoblast cell growth. Trophoblast proliferation contributes to establishing the maternal-fetal interface. It was assessed whether miR-20b-5p, miR-155-5p and miR-718 inhibitor affected trophoblast cell growth. The immortalized human trophoblast HTR8 cell line was used in the present study. Overexpression of miR-20b-5p and inhibition of miR-718 did not affect HTR8 cell growth; however, when cells overexpressed miR-155-5p, the number of cells was significantly reduced and apoptotic bodies were observed, suggesting that miR-155-5p inhibited trophoblast cell growth (Fig. 2A and B). The levels of cyclins affect cell cycle progression; therefore, the expression levels of different cyclins were assessed. Overexpression of miR-155-5p did not affect the expression levels of cyclin A and cyclin D; however, the levels of cyclin E were reduced, and this phenotype was rescued by co-transfecting cells with the miR-155-5p inhibitor (Fig. 2D). The expression levels of miR-155-5p were also confirmed by performing RT-qPCR (Fig. 2C). These findings indicated that miR-155-5p reduced the expression of cyclin E. Cyclin E regulates S phase entry (23); therefore, whether miR-155-5p decreases the ability of HTR8 cells to enter the S phase was assessed by EdU incorporation assay. Overexpression of miR-155-5p reduced the proportion of EdU^+ cells, and this phenotype was rescued by co-transfecting cells with the miR-155-5p inhibitor (Fig. 2E and F). Thus, miR-155-5p may reduce the S phase entry of HTR8 cells. The ability of cells to enter the M phase was next examined by assessing the mitotic index. Overexpression of miR-155-5p reduced the mitotic index of HTR8 cells, and this was rescued by co-transfecting cells with miR-155-5p inhibitor (Fig. 2G). Taken together, miR-155-5p inhibited trophoblast HTR8 cell growth by reducing S phase and M phase entry.

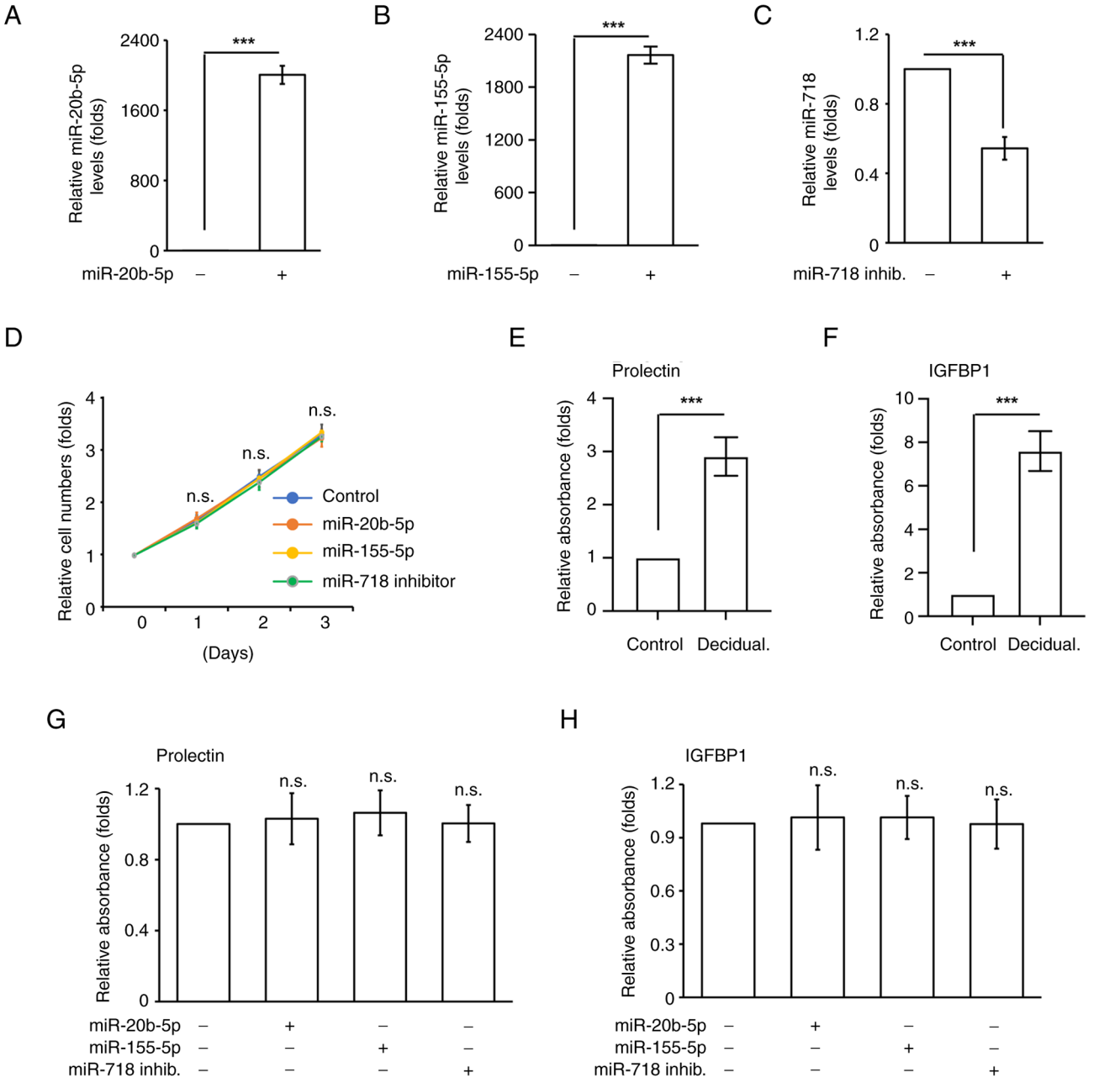

Figure 1. miR-155-5p, miR-20b-5p and miR-718 inhibitor do not affect uterine endometrial stroma cell growth and function. Expression levels of (A) miR-155-5p, (B) miR-20b-5p and (C) miR-718. Quantitative results of cells transfected with miR-155-5p, miR-20b-5p, or miR-718 inhib. (D) Overexpression of miR-155-5p, miR-20b-5p or miR-718 inhibitor did not affect uterine endometrial stroma cell growth. Quantitative results of relative cell numbers of human uterine endometrial stroma cells transfected with miR-155-5p, miR-20b-5p or miR-718 inhib. for 1, 2 and 3 days. (E-H) Overexpression of miR-155-5p, miR-20b-5p or miR-718 inhib. do not affect uterine stroma decidualization. (E and F) Treatment of cAMP and MPA induced uterine stroma decidualization. Decidual markers (E) prolactin and (F) IGFBP1 were upregulated when treating cells with cAMP + MPA. (G and H) Overexpression of miR-155-5p, miR-20b-5p or miR-718 inhib. does not affect (G) prolactin and (H) IGFBP1 levels during decidualization. Data are presented as mean ± SD from three independent experiments. (***P<0.001). All '-' symbols in the figure represent the negative control transfection. n.s., no significance; inhib., inhibitor; cAMP, cyclic adenosine monophosphate; MPA, medroxyprogesterone 17-acetate; IGFBP1, insulin-like growth factor binding protein-1.

In addition to cell cycle progression, some apoptotic bodies were observed in miR-155-5p-overexpressing cells; therefore, cell apoptosis was assessed. Cleaved-caspase 3 and cleaved-PARP, which are markers of apoptosis, were examined in miR-155-5p-overexpressing cells. Overexpression of miR-155-5p increased the levels of cleaved-caspase 3 and cleaved-PARP (Fig. 3A and B), and this phenotype was rescued by co-transfection with the miR-155-5p inhibitor. These data suggested that miR-155-5p induced cell apoptosis.

Overexpression of miR-155-5p induces centrosome amplification. Aberrant mitosis triggers cell apoptosis (36); therefore, whether miR-155-5p-induced apoptosis by aberrant mitosis was assessed. The mitotic spindle poles were examined by staining cells with γ-tubulin. Under normal conditions, cells contained two mitotic spindle poles and the chromosomes were aligned in the middle of the cells (Fig. 3C, left panel); however, when cells overexpressed miR-155-5p, multiple mitotic spindle poles (>2 γ-tubulin spots) and misaligned

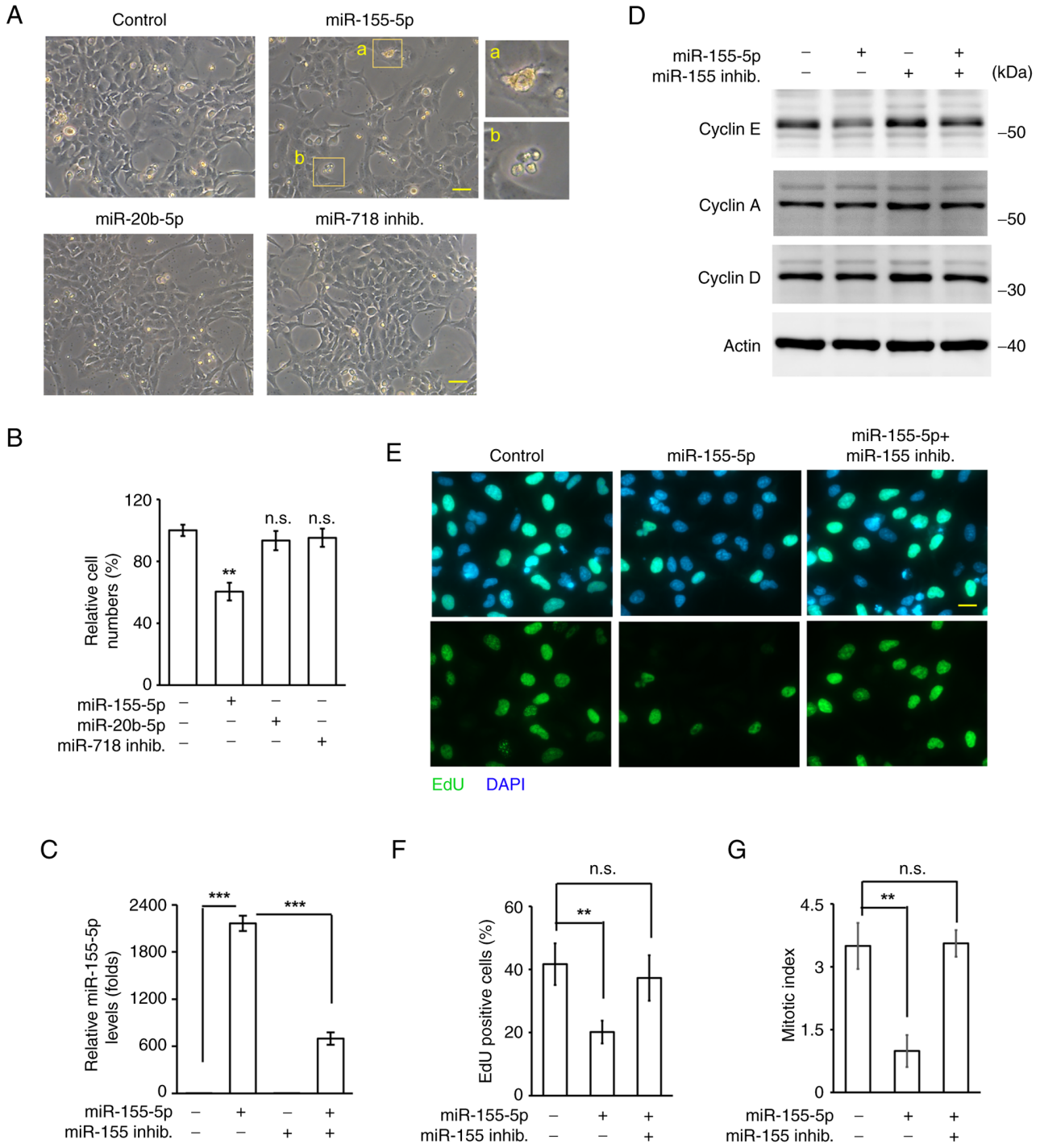

Figure 2. miR-20b-5p inhibits trophoblast HTR8 cell migration and invasion. (A and B) Overexpression of miR-155-5p inhibits HTR8 cell growth. (A) Overexpression of miR-155-5p, not miR-20b-5p or miR-718 inhib., reduced trophoblast HTR8 cell growth. Enlarged views of a and b are apoptotic bodies. Scale bar, 20 μm (B) Quantitative results of (A). (C) Relative levels of miR-155-5p in miR-155-5p with or without miR-155-5p overexpressing cells. (D) Cyclin E levels reduced in miR-155-5p-overexpressing cells. Extracts of miR-155-5p or miR-155-5p inhib. transfected cells were analyzed by western blotting with antibodies against cyclin E, cyclin A, cyclin D and actin (loading control). Overexpression of miR-155-5p reduced S phase entry. (E) EdU-positive cells were reduced in miR-155-5p-overexpressing cells. Scale bar, 10 μm. (F) Quantitative results of (E). (G) Overexpression of miR-155-5p reduced M phase entry. Mitotic index was reduced in miR-155-5p-overexpressing cells. Data are presented as mean ± SD from three independent experiments (**P<0.01, ***P<0.001). All '-' symbols in the figure represent the negative control transfection. n.s., no significance; inhib., inhibitor; HTR8, HTR-8/SVneo.

chromosomes were observed (Fig. 3C, right panel; and Fig. 3D). This phenotype was rescued when cells were co-transfected with the miR-155-5p inhibitor (Fig. 3D). Thus, these data suggested that miR-155-5p triggered aberrant mitosis. Aberrant mitosis is caused by centrosome amplification (cells with >3 centrosomes) during interphase (37); therefore, the centrosome copy numbers during interphase were next assessed. Under normal conditions, cells contained two centrosomes (Fig. 3E, left panel); however, overexpression of miR-155-5p induced centrosome amplification (Fig. 3E, right panel). Co-transfection with the miR-155-5p inhibitor alleviated miR-155-5p-induced centrosome amplification

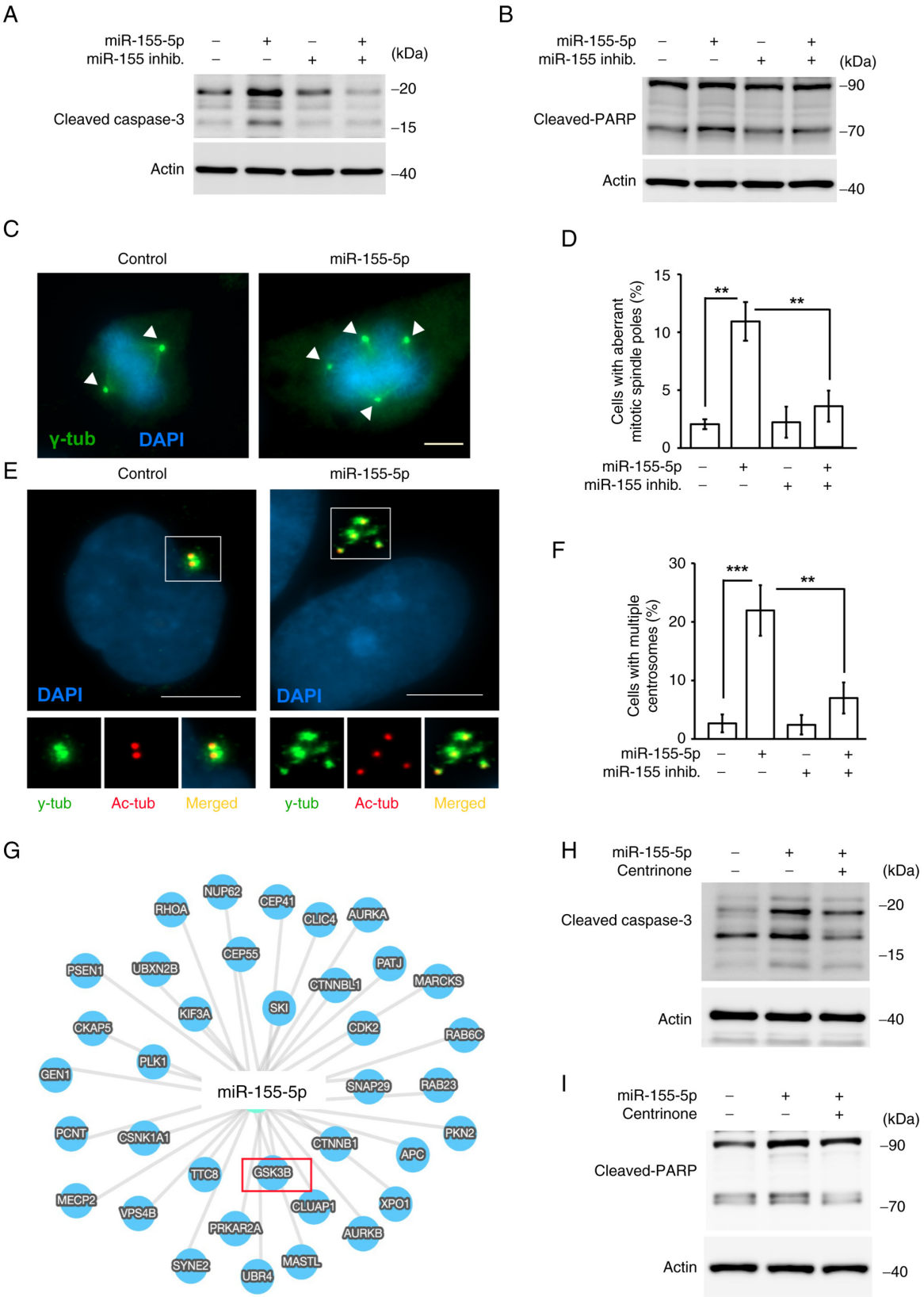

Figure 3. Overexpression of miR-155-5p facilitates centrosome amplification and cellular apoptosis. (A and B) Overexpression of miR-155-5p induced apoptosis. Markers of cellular apoptosis, (A) cleaved-caspase 3 and (B) cleaved-PARP, were examined by western blotting in the presence of miR-155-5p or miR-155-5p inhib. (C and D) Overexpression of miR-155-5p leads to aberrant mitotic spindle poles. (C) Immunofluorescence staining of control or miR-155-5p-overexpressing cells with antibody against γ-tub (green). The arrowhead indicates mitotic spindle poles. DNA was stained with DAPI (scale bar, 5 μm). (D) Quantitative results of (C). (E) Immunofluorescence staining of control, miR-155-5p-, or miR-155-5p inhib.-overexpressing cells with antibodies against acetylated tubulin (centrioles, red) and γ-tub (pericentriolar material, green). DNA was stained with DAPI (scale bar, 10 μm). (F) Quantitative results of (E). (G) GSK3β was a putative candidate of miR-155-5p targeted gene shown by in silicon prediction. (H-I) Inhibition of centrosome amplification by treating cells with centrinone reduced cellular apoptosis. Extracts of miR-155-5p-overexpressing cells in the presence or absence of centrinone were analyzed by western blotting assay with antibodies against (H) cleaved-caspase 3, (I) cleaved-PARP or actin. Data are presented as mean ± SD from three independent experiments (**P<0.01, ***P<0.001). inhib., inhibitor; PARP, poly (ADP-ribose) polymerase; γ-tub, γ-tubulin; Ac-tub, acetylated tubulin.

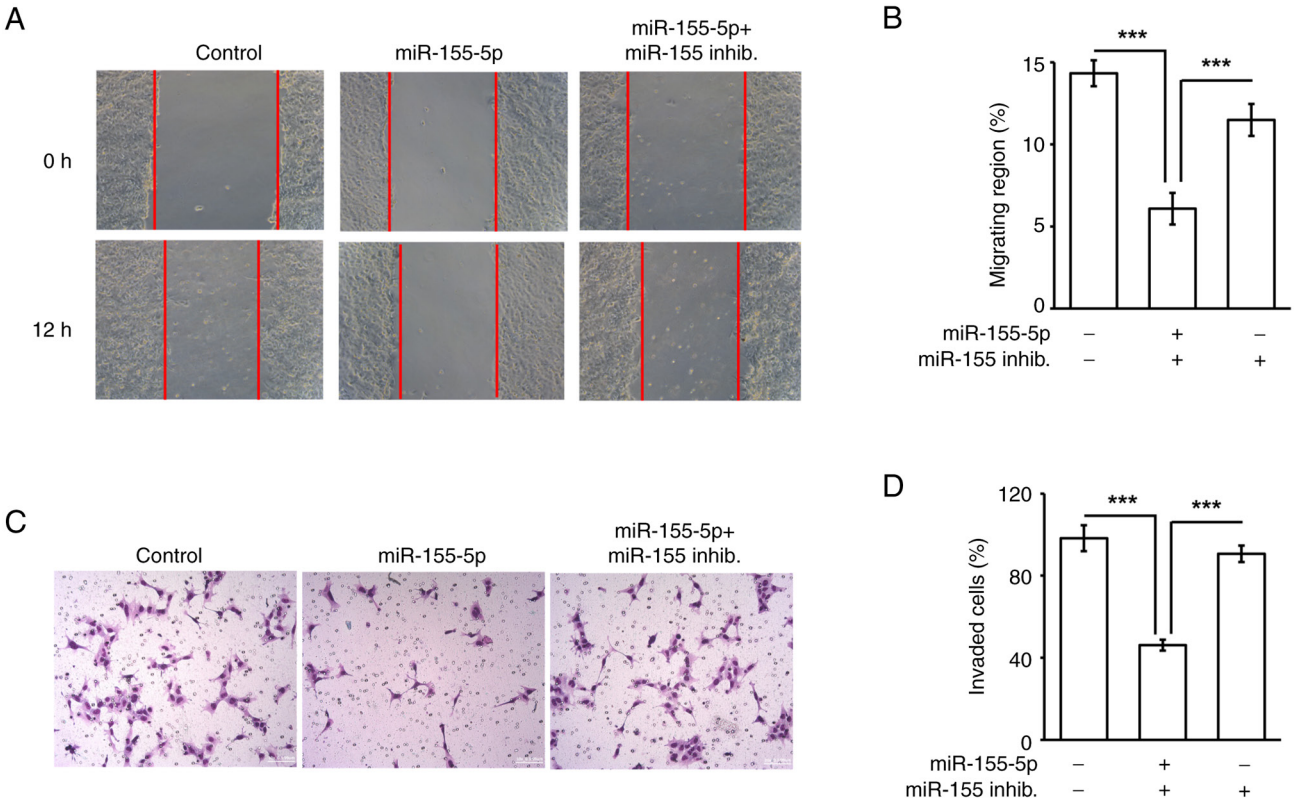

Figure 4. Overexpression of miR-155-5p inhibits trophoblast cell migration and invasion. (A and B) Overexpression of miR-155-5p inhibits trophoblast cell migration. (A) Ability of HTR8 migration was detected 0 h or 12 h after scratching in control, miR-155-5p or miR-155 inhib. transfected cells. Magnification, x40X. (B) Quantitative results of (A). (C and D) Overexpression of miR-155-5p inhibits HTR8 cell invasion. (C) After miRNAs transfection, Matrigel invasion assay was performed, and invaded cells were observed by light microscope. Magnification: 200X. (D) Quantitative results of (C). Data are presented as mean ± SD from three independent experiments (***P<0.00). inhib., inhibitor; HTR8, HTR-8/SVneo.

(Fig. 3F), supporting the hypothesis that miR-155-5p induced centrosome amplification. Whether centrosome amplification contributed to apoptosis upon miR-155-5p overexpression was next examined. Overexpression of miR-155-5p increased the levels of cleaved-caspase 3 and cleaved-PARP; however, inhibition of centrosome amplification by treating cells with the centrosome inhibitor centrinone rescued these phenotypes (Fig. 3H and I), suggesting that centrosome amplification promoted cell death. Using bioinformatics analysis, several genes, such as GSK3β, PLK3, or KIF3A, were predicted as the targets of miR-155-5p. GSK3β was identified as a putative candidate of miR-155-5p (Fig. 3G). A previous study showed that the downregulation of GSK3β led to the accumulation of β-catenin followed by induction of centrosome amplification (38,39). Thus, miR-155-5p may target GSK3β to induce centrosome amplification. Taken together, miR-155-5p induced centrosome amplification, thus triggering trophoblast cell apoptosis.

Overexpression of miR-155-5p inhibits trophoblast migration and invasion. Trophoblast cell migration and invasion are critical for placenta formation during early pregnancy (30); thus whether overexpression of miR-155-5p impeded trophoblast migration and invasion was examined. Since miR-155-5p inhibited HTR8 cell growth, seeding cell numbers were adjusted according to the growth assay. A total of $5x10^5$ control and $7x10^5$ miR-155-5p-transsfected cells were seeded to perform the migration and invasion assays. First, the effects of miR-155-5p on trophoblast cell migration was assessed by performing a wound healing assay. Overexpression of miR-155-5p inhibited trophoblast cell migration, and this phenotype was rescued by co-transfecting cells with the miR-155-5p inhibitor (Fig. 4A and B), suggesting that upregulation of miR-155-5p reduced trophoblast cell migration. Next, trophoblast cell invasion was examined. Consistent with the results of the cell migration assay, the invasive ability of trophoblast cells was reduced by miR-155-5p overexpression (Fig. 4C and D), suggesting that miR-155-5p inhibited cell invasion. Collectively, miR-155-5p inhibited HTR8 trophoblast cell migration and invasion. EMT is key for trophoblast cell invasion during early pregnancy (18). Since miR-155-5p inhibited trophoblast cell invasion, the EMT was examined in the present study. In miR-155-5p-overexpressing cells, the epithelial marker E-cadherin was increased, whereas the mesenchymal markers ZEB-1, fibronectin-1 and THBS1 were significantly decreased, suggesting that miR-155-5p inhibited EMT (Fig. 5A-D). By contrast, co-transfection with the miR-155-5p inhibitor rescued the expression levels of the EMT markers. Taken together, miR-155-5p inhibited trophoblast cell invasion by reducing EMT.

Overexpression of miR-155-5p inhibits p38 activation and primary ciliogenesis. Primary cilia promote trophoblast cell invasion; therefore, whether miR-155-5p affected primary cilia formation was assessed. HTR8 cells grew primary cilia, as evidenced by several markers, including markers of the

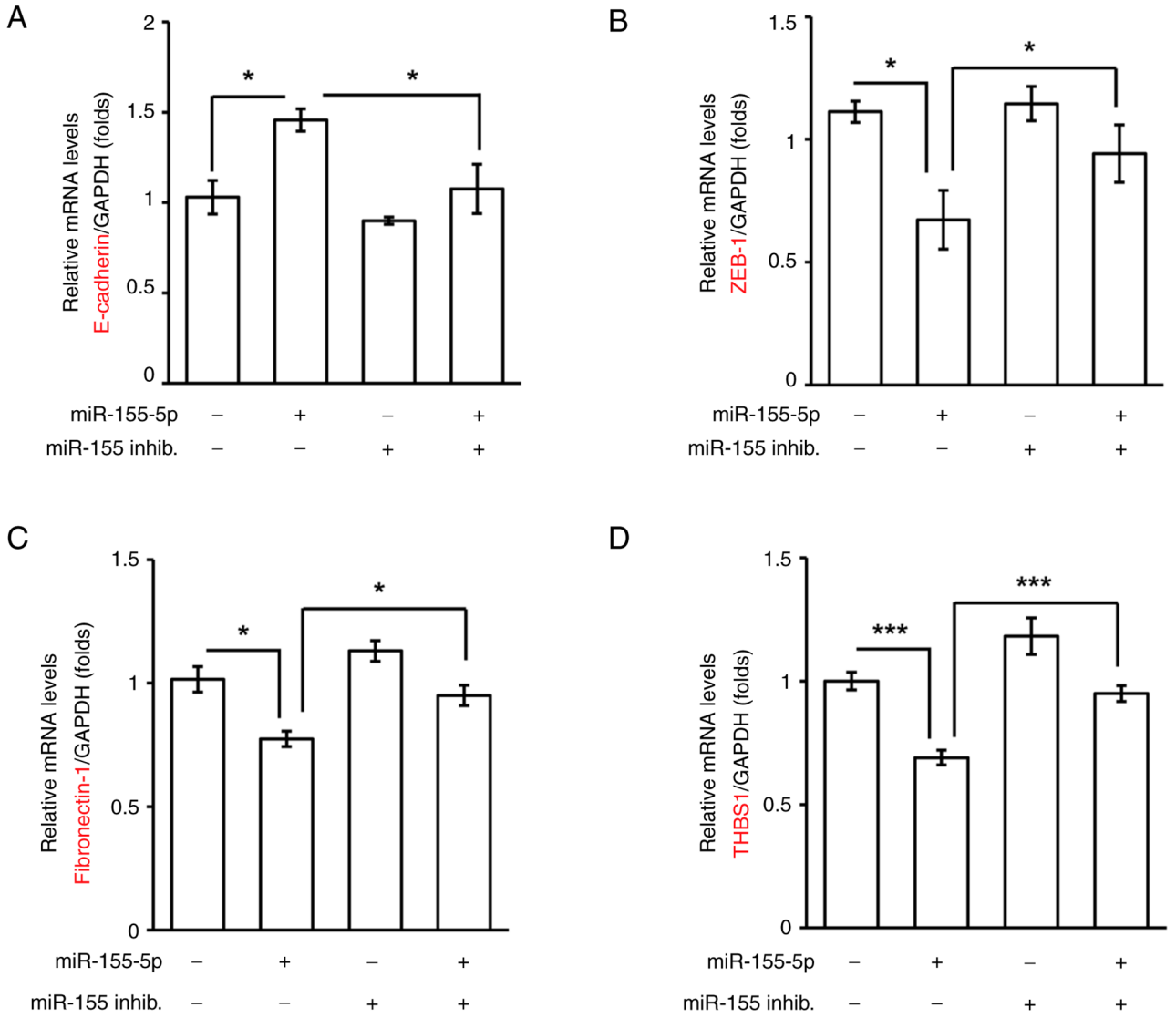

Figure 5. miR-155-5p inhibits the EMT and MMP2 of trophoblast cells. (A-D) Overexpression of miR-155-5p inhibited EMT of HTR8 cells. mRNA levels of (A) epithelial marker E-cadherin increased and (B) mesenchymal marker ZEB-1, (C) fibronectin-1 and (D) THBS1 decreased as detected using RT-qPCR. GAPDH was used as the internal control. Data are presented as mean ± SD from three independent experiments (*P<0.05, ***P<0.001). EMT, epithelial-mesenchymal transition; MMP2, matrix metalloproteinase 2; ZEB-1, zinc-finger E-box-binding homeobox 1; THBS1, thrombospondin 1; HTR8, HTR-8/SVneo; inhib., inhibitor.

axoneme (acetylated tubulin), ciliary membrane (ARL13B), intraflagellar transporter (IFT88) and basal body (CEP164; Fig. 6A-C). Overexpression of miR-155-5p reduced the proportions of ciliated cells, and this phenotype was rescued by co-transfection of cells with the miR-155-5p inhibitor (Fig. 6D and E). These data suggested that miR-155-5p reduced primary cilia formation. Next, which signaling contributed to primary cilia formation was assessed. AKT, ERK and p38 are known to regulate primary cilia formation; therefore it was next assessed whether these signaling pathways were activated and participated in miR-155-5p-mediated primary cilia formation. Overexpression of miR-155-5p did not affect AKT and ERK activation; however, phospho-p38 (active form) was reduced, and this phenotype was rescued by co-transfecting cells with the miR-155-5p inhibitor (Fig. 7A-C). Thus, miR-155-5p inhibited p38 activation. It was then examined whether p38 reduced primary cilia formation. HTR8 cells grew primary cilia; however, in response to treatment of HTR8 cells with the p38 inhibitor SB203580, the proportions of ciliated cells were decreased (Fig. 7D). It was also observed that the p38 inhibitor reduced invasive ability (Fig. 7E), suggesting that p38 activity was required for trophoblast invasion. To confirm this finding further, miR-155-5p-overexpressing cells were treated with the p38 activator and found activation of p38 restored the primary cilia formation and invasive ability (Fig. 7F and G). Taken together, miR-155-5p inactivated p38, thus reducing primary cilia formation and trophoblast invasion.

Overexpression of miR-155-5p regulates autophagy in trophoblast cells. Autophagic homeostasis maintains trophoblast cell growth and invasion. It was then checked whether autophagy is mediated by miR-155-5p. The levels of LC3 II were increased in miR-155-5p-overexpressing cells, whereas this phenotype was rescued by co-transfection with the miR-155-5p inhibitor, suggesting that miR-155-5p induced

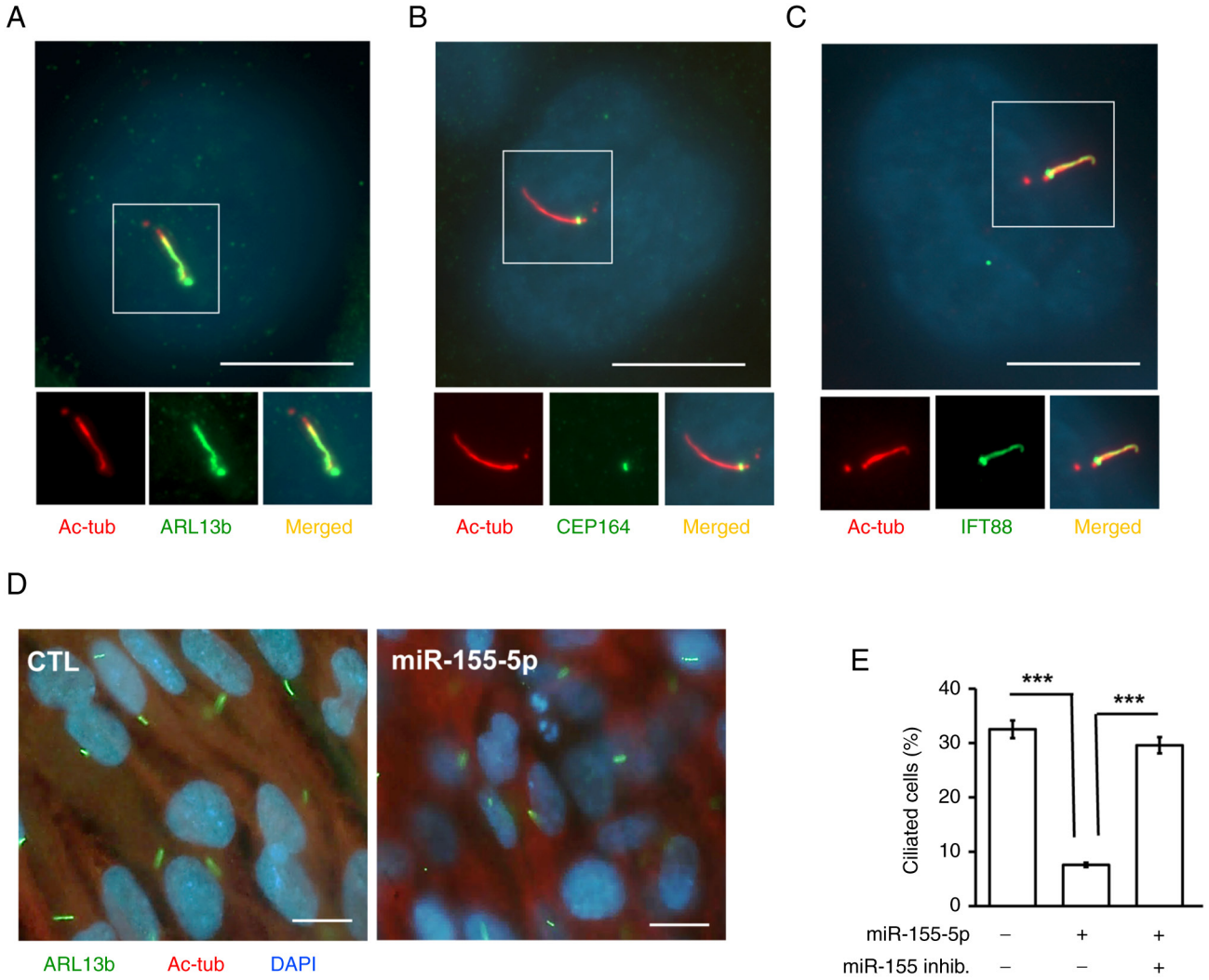

Figure 6. Overexpression of miR-155-5p inhibits primary cilia formation. (A) ARL13b (marker of ciliary membrane). (B) CEP164 (marker of basal body) and (C) IFT88 (marker of intraflagella). DNA was stained with DAPI (blue; scale bar, 5 μm). (D and E) miR-155-5p inhibited primary cilia formation. (D) Immunofluorescence staining of primary cilia with antibodies against ARL13b and Ac-tub in the presence or absence of miR-155-5p. (E) Quantitative results of (D). Data are presented as mean ± SD from three independent experiments (***P<0.001). Ac-tub, acetylated tubulin; inhib., inhibitor; ARL13b, ADP-ribosylation factor-like 13B; CEP164, centrosomal protein 164; IFT88, intraflagellar transport 88.

autophagy (Fig. 8A). Next, whether autophagy contributed to cell death was assessed. ATG16L1, an important regulator of autophagy, was depleted by transfecting HTR8 cells with siRNA against ATG16L1 (Fig. 8B). In addition, the cell death and cell cycle pathways were examined. Depletion of ATG16L1 reduced cleaved-caspase 3 and cleaved-PARP, whereas the cyclin E expression was increased in ATG16L1-deficient cells (Fig. 8C and D). These data indicated that autophagy triggered cell death and inhibited cell cycle progression. Degradation of the extracellular matrix by MMP2 promotes cell invasion; therefore, the effect of miR-155-5p on MMP2 expression was examined. Overexpression of miR-155-5p reduced the mRNA and protein expression levels of MMP2, whereas co-transfection with the miR-155-5p inhibitor rescued the expression of MMP2 (Fig. 8E and F). Thus, miR-155-5p may inhibit MMP2 expression. Next, whether MMP2 was regulated by autophagy was assessed. The levels of MMP2 were increased in ATG16L1-deficient cells (Fig. 8D), suggesting that autophagy inhibited cell invasion. To confirm whether autophagy regulated trophoblast cell growth and invasion, autophagy was inhibited by treating cells with the selective inhibitor of autophagy, 3-methyladenine (3-MA). Treatment with 3-MA induced HTR8 cell invasion (Fig. 8G). These data suggested that autophagy is required for trophoblast cell growth and invasion. Taken together, miR-155-5p induced autophagy, reducing cell growth and invasion.

Discussion

Recurrent miscarriage leads to infertility in women, and defective trophoblast cell growth and invasion are major causes of recurrent miscarriage (1,40). Dysregulation of miR-155-5p has been identified in women with recurrent miscarriage; however, the underlying molecular mechanisms remain to be elucidated. In the present study, it was demonstrated that miR-155-5p blocked trophoblast cell growth and invasion by affecting centrosome homeostasis and primary cilia formation, and overexpression of miR-155-5p induced centrosome amplification, followed by the promotion of cell death. Furthermore, miR-155-5p inhibited primary cilia formation

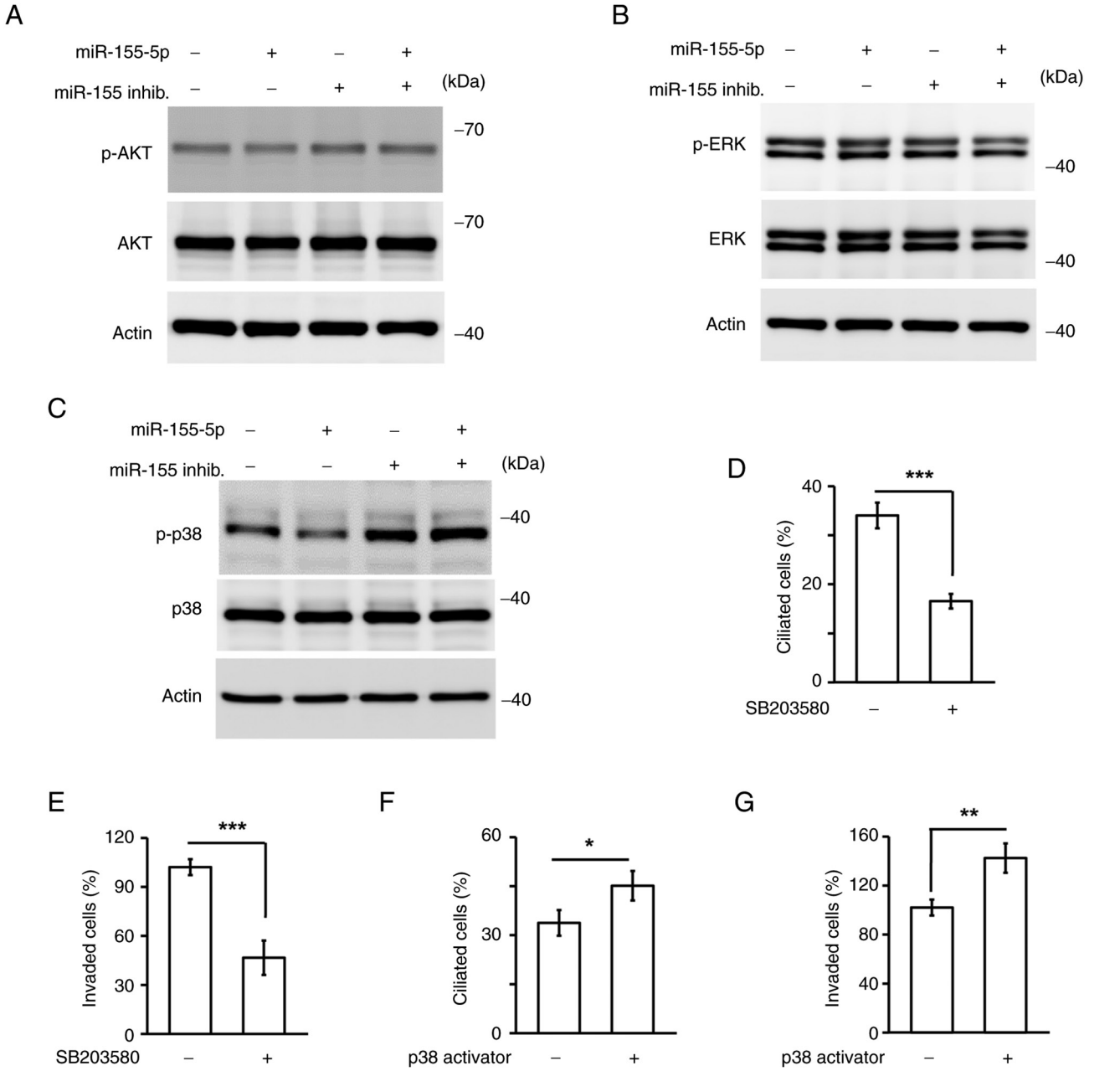

Figure 7. miR-155-5p inhibits primary cilia by blocking p38 activation. (A-C) Overexpression of miR-155-5p reduced p38, but not AKT and ERK, activation. Extracts of cells transfected with miR-155-5p or miR-155-55p inhib. were analyzed by western blotting with antibodies against (A) p-AKT at Ser473 and Akt or (B) p-ERK at Thr202/Tyr204 and ERK or (C) p-p38 at Thr180/Tyr182 and p38. (D) Inhibition of p38 by treating cells with SB203580 reduced primary cilia formation. Quantitative results of ciliated cells (%) in the presence of miR-155-5p or miR-155-5p inhib. (E) Inhibition of p38 reduced cell invasion. Quantitative results of invaded cells (%) in the presence of SB203580. (F and G) Activation of p38 induced primary cilia (F) formation and (G) cell invasion. Data are presented as mean ± SD from three independent experiments (*P<0.05, **P<0.01, ***P<0.001). p-, phosphorylated; inhib., inhibitor.

by reducing p38 activation, thus inhibiting trophoblast cell invasion. Notably, these events were regulated by autophagy (Fig. 9). Thus, the potential molecular mechanisms by which miR-155-5p contributes to recurrent miscarriage may have been elucidated.

The present study found that miR-155-5p inactivated p38, thus reducing primary cilia formation; however, the link between p38 activation and primary cilia formation remains less studied. Sex-determining region Y-box 9 (SOX9) belongs to the SOX transcription factor family. SOX9 maintains organ development and differentiation during mammalian embryo development (41). Recent studies have shown that SOX9 also participates in controlling primary cilia formation (42,43). Primary cilia are markedly reduced in SOX9-knockout mice, implying that SOX9 maintains primary cilia formation (44). Notably, p38 activation maintains the mRNA stability of SOX9 (45). Furthermore, depletion or inhibition of p38 via siRNA alleviates the phosphorylation and protein stability of SOX9, supporting the hypothesis that p38 activation is crucial for SOX9 expression and activation (45). In the present study, miR-155-5p inhibits p38 activation and inhibition of p38 reduced primary cilia formation in trophoblast cells. It was therefore hypothesized that miR-155-5p may inactivate p38, thus reducing SOX9 expression and inhibiting primary cilia

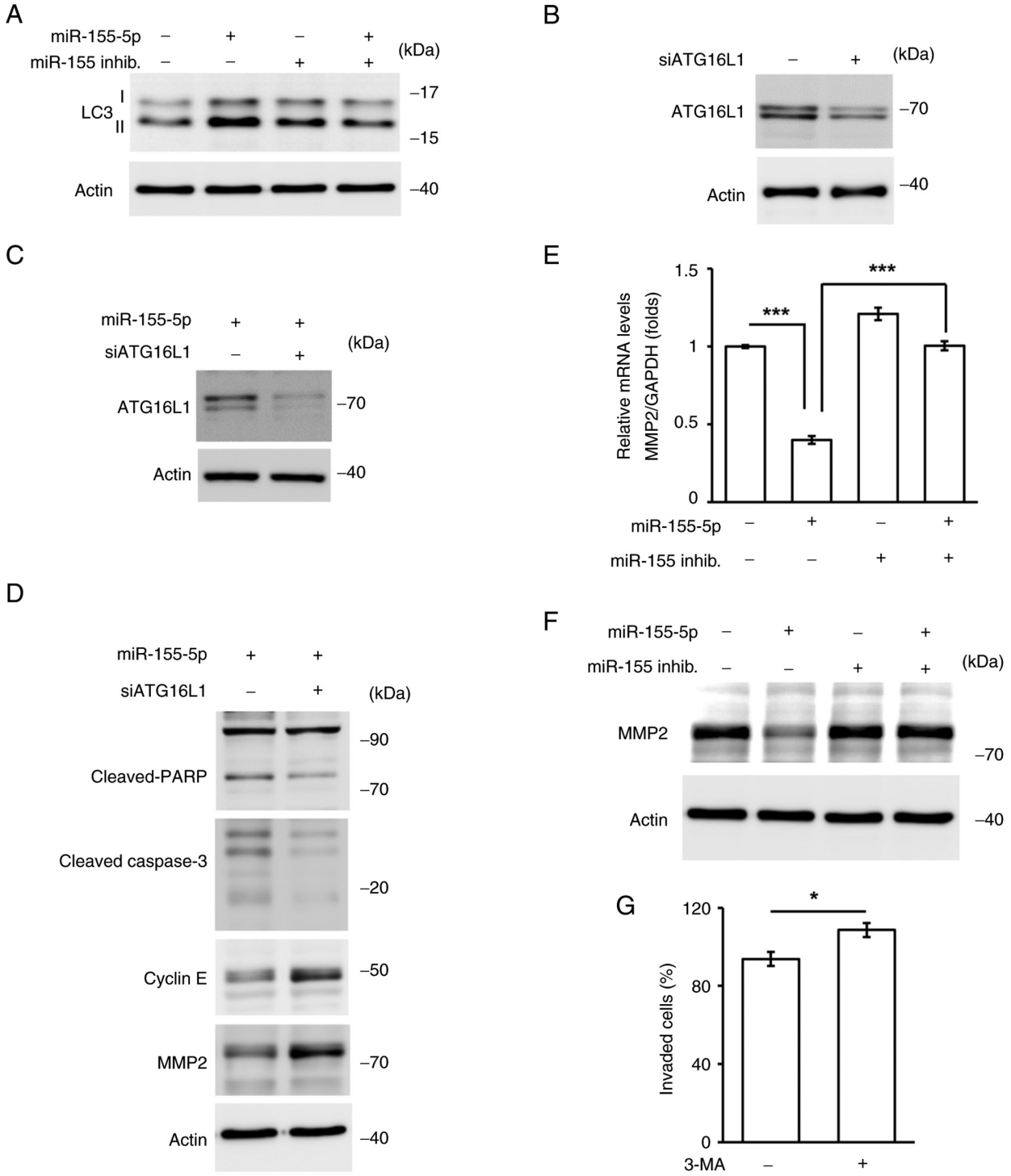

Figure 8. miR-155-5p regulates autophagy for trophoblast cell growth and invasion. (A) Overexpression of miR-155-5p induced autophagy. Extracts of miR-155-5p- or miR-155-5p inhibitor-transfecting cells were analyzed by western blotting assay with antibodies against LC3I/II and actin. (B-D) Autophagy inhibited trophoblast cell growth and invasion. (B-C) ATG16L1 was depleted efficiently. Extracts of cells transfected with siRNA against ATG16L1 in the (B) absence or (C) presence of miR-155-5p were analyzed with antibodies against ATG16L1 and actin. (D) Depletion of ATG16L1 inhibited cell apoptosis and promoted MMP2 expressions. Extraction of ATG16L1-depleting HTR8 cells were analyzed by western blotting with antibodies against cleaved-caspase 3, cleaved-PARP, cyclin E, MMP2 and actin. (E and F) Overexpression of miR-155-5p inhibited MMP2 expression. (E) mRNA levels of MMP2 were reduced in miR-155-5p-transfected cells. (F) Protein levels of MMP2 were reduced in miR-155-5p-overexpressing HTR8 cells. Extracts of miR-155-5p or miR-155-5p inhib. transfected cells were analyzed by western blotting with antibodies against MMP2 and actin (loading control). (G) Treatment of cells with 1 mM 3-MA induced cell invasion. All experiments were repeated at least for three times. *P<0.05, ***P<0.001. All '-' symbols in the figure represent the negative control transfection. inhib., inhibitor; LC3I/II, light chain 3 I/II; ATG16L1, autophagy-related 16-like 1; HTR8, HTR-8/SVneo; PARP, poly (ADP-ribose) polymerase; 3-MA, 3-methyladenine.

formation. This hypothesis requires further confirmation in the future.

During the progression of glioma, the exosomes secreted by glioma stem-like cells contain a high abundance of

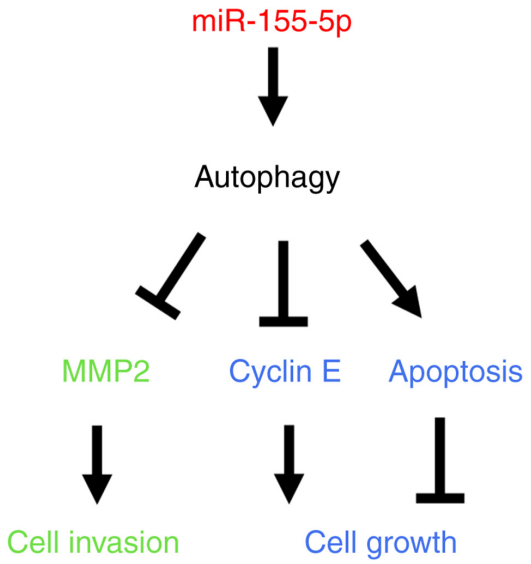

Figure 9. Schematic overview of miR-155-5p regulation of trophoblast cell proliferation and invasion. miR-155-5p inhibits trophoblast cell growth by inducing cell apoptosis and blocking cyclin E expression. In addition, miR-155-5p reduces trophoblast invasion by reducing MMP2 expression. These events are regulated by autophagy.

miR-155-5p. These miR-155-5p-containing exosomes are taken up by the glioma and suppress the levels of acetyl-CoA thioesterase 12, a tumor suppressor, thus promoting glioma cell proliferation (46). By contrast, high miR-155-5p levels reduce hepatocellular carcinoma cell growth (47). By targeting collagen triple helix repeat-containing 1, miR-155-5p can inhibit cell cycle progression, invasion and migration, and promote cellular apoptosis *in vitro* and *in vivo* (47). In addition, miR-155-5p indirectly modulates the malignancy of liver cancer by regulating Wnt/β-catenin signaling (47). The present study showed that miR-155-5p inhibited cell cycle progression and induced apoptosis in trophoblast cells; however, miR-155-5p inhibited trophoblast cell invasion for placenta formation by inhibiting the EMT and MMP2 expression. Thus, miR-155-5p may serve contradictory roles in different tissues. In glioma or triple-negative breast cancer, miR-155-5p promotes cell growth; however, miR-155-5p inhibits liver cancer and trophoblast cell proliferation and invasion (16,48). These data imply that distinct targeted genes or regulatory complexes may cause the tissue type-specific functions of miR-155-5p. Future studies should focus on clarifying and identifying the underlying distinct molecular mechanisms.

Preeclampsia is characterized by hypertension and proteinuria during pregnancy (16). Patients with preeclampsia suffer from organ dysfunction and the symptoms end after delivery (16). During pregnancy, trophoblast cells invade the maternal decidua and remodel the uterine spiral arteries to increase uteroplacental blood perfusion (40). Insufficient invasion of trophoblast cells causes preeclampsia; notably, upregulation of miR-155-5p is associated with preeclampsia (49). The expression of miR-155-5p has been shown to be increased in preeclamptic placentas compared with the control group (49); however, the underlying molecular mechanism remains unclear. The present study demonstrated that upregulation of miR-155-5p reduced trophoblast invasion by reducing primary cilia formation. Furthermore, previous studies have shown that loss of primary cilia is observed in the preeclamptic placentas (18,30). It was thus speculated that, during the progression of preeclampsia, upregulation of miR-155-5p may inhibit trophoblast cell EMT and invasion, therefore reducing the establishment of maternal-fetal interfaces; therefore, targeting miR-155-5p may be a good strategy to reduce the severity of preeclampsia or prevent recurrent miscarriage.

The data are obtained from *in vitro* cell culture models. To overcome this limitation and further confirm the pathophysiological role of miR-155-5p, the miR-155-5p-overexpressed transgenic mice can be generated and examine the implantation and pregnancy *in vivo*.

In conclusion, the present study uncovered the role of miR-155-5p in contributing to recurrent miscarriage. Overexpression of miR-155-5p induced centrosome amplification, thus reducing cell cycle progression and inducing cellular apoptosis. In addition, miR-155-5p reduced primary cilia formation, thereby inhibiting EMT and trophoblast invasion. Thus, miR-155-5p not only functions as a biomarker of recurrent miscarriage but may be considered a good candidate to prevent recurrent miscarriage.

Acknowledgements

The authors would like to thank Ms. Pey-Wen Liu (Core Research Laboratory, College of Medicine, National Cheng Kung University, Tainan, Taiwan) for technical support.

Funding

The present study was supported by the Ministry of Science and Technology of Taiwan (MOST109-2320-B-006-042-MY3 and NSTC112-2320-B-006-040) and the Chi Mei Medical Center (CMNCKU11108).

Availability of data and materials

The data generated in the present study are included in the figures and/or tables of this article.

Authors' contributions

PJS and CYW conceived the study and wrote, reviewed and edited the manuscript. YCT, TNK, RCL, HLT, YYC and PRL designed experiments. YCT, TNK, HLT, YYC and PRL performed experiments. RCL, HLT and YYC analyzed data. YCT and RCL wrote, reviewed and edited the manuscript. All authors have read and approved the final manuscript. CYW and RCL confirm the authenticity of all the raw data.

Ethics approval and consent to participate

Not applicable.

Patient consent for publication

Not applicable.

Competing interests

The authors declare that they have no competing interests.

References

1. Bashiri A, Halper KI and Orvieto R: Recurrent implantation failure-update overview on etiology, diagnosis, treatment and future directions. Reprod Biol Endocrinol 16: 121, 2018.
2. Ford HB and Schust DJ: Recurrent pregnancy loss: Etiology, diagnosis, and therapy. Rev Obstet Gynecol 2: 76-83, 2009.
3. Rai R and Regan L: Recurrent miscarriage. Lancet 368: 601-611, 2006.
4. You Y, Stelzl P, Joseph DN, Aldo PB, Maxwell AJ, Dekel N, Liao A, Whirledge S and Mor G: TNF-α regulated endometrial stroma secretome promotes trophoblast invasion. Front Immunol 12: 737401, 2021.
5. Zhang S, Lin H, Kong S, Wang S, Wang H, Wang H and Armant DR: Physiological and molecular determinants of embryo implantation. Mol Aspects Med 34: 939-980, 2013.
6. Pan-Castillo B, Gazze SA, Thomas S, Lucas C, Margarit L, Gonzalez D, Francis LW and Conlan RS: Morphophysical dynamics of human endometrial cells during decidualization. Nanomedicine 14: 2235-2245, 2018.
7. Vento-Tormo R, Efremova M, Botting RA, Turco MY, Vento-Tormo M, Meyer KB, Park JE, Stephenson E, Polański K, Goncalves A, *et al*: Single-cell reconstruction of the early maternal-fetal interface in humans. Nature 563: 347-353, 2018.
8. Carter AM, Enders AC and Pijnenborg R: The role of invasive trophoblast in implantation and placentation of primates. Philos Trans R Soc Lond B Biol Sci 370: 20140070, 2015.
9. Meakin C, Barrett ES and Aleksunes LM: Extravillous trophoblast migration and invasion: Impact of environmental chemicals and pharmaceuticals. Reprod Toxicol 107: 60-68, 2022.
10. Ambros V: The functions of animal microRNAs. Nature 431: 350-355, 2004.
11. Jouravleva K, Golovenko D, Demo G, Dutcher RC, Hall TMT, Zamore PD and Korostelev AA: Structural basis of microRNA biogenesis by Dicer-1 and its partner protein Loqs-PB. Mol Cell 82: 4049-4063.e6, 2022.
12. Basavarajappa D, Uebbing S, Kreiss M, Lukic A, Suess B, Steinhilber D, Samuelsson B and Rådmark O: Dicer up-regulation by inhibition of specific proteolysis in differentiating monocytic cells. Proc Natl Acad Sci USA 117: 8573-8583, 2020.
13. Muys BR, Sousa JF, Plaça JR, de Araújo LF, Sarshad AA, Anastasakis DG, Wang X, Li XL, de Molfetta GA, Ramão A, *et al*: miR-450a acts as a tumor suppressor in ovarian cancer by regulating energy metabolism. Cancer Res 79: 3294-3305, 2019.
14. Singh R, Yadav V, Kumar S and Saini N: MicroRNA-195 inhibits proliferation, invasion and metastasis in breast cancer cells by targeting FASN, HMGCR, ACACA and CYP27B1. Sci Rep 5: 17454, 2015.
15. Sun Z, Shi K, Yang S, Liu J, Zhou Q, Wang G, Song J, Li Z, Zhang Z and Yuan W: Effect of exosomal miRNA on cancer biology and clinical applications. Mol Cancer 17: 147, 2018.
16. Skalis G, Katsi V, Miliou A, Georgiopoulos G, Papazachou O, Vamvakou G, Nihoyannopoulos P, Tousoulis D and Makris T: MicroRNAs in preeclampsia. Microrna 8: 28-35, 2019.
17. Zhang H, He Y, Wang JX, Chen MH, Xu JJ, Jiang MH, Feng YL and Gu YF: miR-30-5p-mediated ferroptosis of trophoblasts is implicated in the pathogenesis of preeclampsia. Redox Biol 29: 101402, 2020.
18. Wang CY, Tsai PY, Chen TY, Tsai HL, Kuo PL and Su MT: Elevated miR-200a and miR-141 inhibit endocrine gland-derived vascular endothelial growth factor expression and ciliogenesis in preeclampsia. J Physiol 597: 3069-3083, 2019.
19. Chen CH, Lu F, Yang WJ, Yang PE, Chen WM, Kang ST, Huang YS, Kao YC, Feng CT, Chang PC, *et al*: A novel platform for discovery of differentially expressed microRNAs in patients with repeated implantation failure. Fertil Steril 116: 181-188, 2021.
20. Lai PY, Wang CY, Chen WY, Kao YH, Tsai HM, Tachibana T, Chang WC and Chung BC: Steroidogenic factor 1 (NR5A1) resides in centrosomes and maintains genomic stability by controlling centrosome homeostasis. Cell Death Differ 18: 1836-1844, 2011.
21. Chen TY, Lien WC, Cheng HL, Kuan TS, Sheu SY and Wang CY: Chloroquine inhibits human retina pigmented epithelial cell growth and microtubule nucleation by downregulating $p150^{glued}$. J Cell Physiol 234: 10445-10457, 2019.
22. Lin RC, Chao YY, Lien WC, Chang HC, Tsai SW and Wang CY: Polo-like kinase 1 selective inhibitor BI2536 (dihydropteridinone) disrupts centrosome homeostasis via ATM-ERK cascade in adrenocortical carcinoma. Oncol Rep 50: 167, 2023.
23. Ferguson RL and Maller JL: Centrosomal localization of cyclin E-Cdk2 is required for initiation of DNA synthesis. Curr Biol 20: 856-860, 2010.
24. Chen TY, Lin TC, Kuo PL, Chen ZR, Cheng HL, Chao YY, Syu JS, Lu FI and Wang CY: Septin 7 is a centrosomal protein that ensures S phase entry and microtubule nucleation by maintaining the abundance of $p150^{glued}$. J Cell Physiol 236: 2706-2724, 2021.
25. Chao YY, Huang BM, Peng IC, Lee PR, Lai YS, Chiu WT, Lin YS, Lin SC, Chang JH, Chen PS, *et al*: ATM- and ATR-induced primary ciliogenesis promotes cisplatin resistance in pancreatic ductal adenocarcinoma. J Cell Physiol 237: 4487-4503, 2022.
26. Hildebrandt F, Benzing T and Katsanis N: Ciliopathies. N Engl J Med 364: 1533-1543, 2011.
27. Yamamoto Y and Mizushima N: Autophagy and ciliogenesis. JMA J 4: 207-215, 2021.
28. Truong ME, Bilekova S, Choksi SP, Li W, Bugaj LJ, Xu K and Reiter JF: Vertebrate cells differentially interpret ciliary and extraciliary cAMP. Cell 184: 2911-2926.e18, 2021.
29. Tsai YC, Kuo TN, Chao YY, Lee PR, Lin RC, Xiao XY, Huang BM and Wang CY: PDGF-AA activates AKT and ERK signaling for testicular interstitial Leydig cell growth via primary cilia. J Cell Biochem 124: 89-102, 2023.
30. Wang CY, Tsai HL, Syu JS, Chen TY and Su MT: Primary cilium-regulated EG-VEGF signaling facilitates trophoblast invasion. J Cell Physiol 232: 1467-1477, 2017.
31. Gu X, Liu H, Luo W, Wang X, Wang H and Li L: Di-2-ethylhexyl phthalate-induced miR-155-5p promoted lipid metabolism via inhibiting cAMP/PKA signaling pathway in human trophoblastic HTR-8/Svneo cells. Reprod Toxicol 114: 22-31, 2022.
32. Graham CH, Hawley TS, Hawley RG, MacDougall JR, Kerbel RS, Khoo N and Lala PK: Establishment and characterization of first trimester human trophoblast cells with extended lifespan. Exp Cell Res 206: 204-211, 1993.
33. Abou-Kheir W, Barrak J, Hadadeh O and Daoud G: HTR-8/SVneo cell line contains a mixed population of cells. Placenta 50: 1-7, 2017.
34. Tan HX, Yang SL, Li MQ and Wang HY: Autophagy suppression of trophoblast cells induces pregnancy loss by activating decidual NK cytotoxicity and inhibiting trophoblast invasion. Cell Commun Signal 18: 73, 2020.
35. Livak KJ and Schmittgen TD: Analysis of relative gene expression data using real-time quantitative PCR and the 2(-Delta Delta C(T)) method. Methods 25: 402-408, 2001.
36. Orth JD, Loewer A, Lahav G and Mitchison TJ: Prolonged mitotic arrest triggers partial activation of apoptosis, resulting in DNA damage and p53 induction. Mol Biol Cell 23: 567-576, 2012.
37. Wang CY, Kao YH, Lai PY, Chen WY and Chung BC: Steroidogenic factor 1 (NR5A1) maintains centrosome homeostasis in steroidogenic cells by restricting centrosomal DNA-dependent protein kinase activation. Mol Cell Biol 33: 476-484, 2013.
38. Bahmanyar S, Guiney EL, Hatch EM, Nelson WJ and Barth AIM: Formation of extra centrosomal structures is dependent on beta-catenin. J Cell Sci 123: 3125-3135, 2010.
39. Wang CY, Lai PY, Chen TY and Chung BC: NR5A1 prevents centriole splitting by inhibiting centrosomal DNA-PK activation and β-catenin accumulation. Cell Commun Signal 12: 55, 2014.
40. Illsley NP, DaSilva-Arnold SC, Zamudio S, Alvarez M and Al-Khan A: Trophoblast invasion: Lessons from abnormally invasive placenta (placenta accreta). Placenta 102: 61-66, 2020.
41. Ming Z, Vining B, Bagheri-Fam S and Harley V: SOX9 in organogenesis: Shared and unique transcriptional functions. Cell Mol Life Sci 79: 522, 2022.
42. Edelman HE, McClymont SA, Tucker TR, Pineda S, Beer RL, McCallion AS and Parsons MJ: SOX9 modulates cancer biomarker and cilia genes in pancreatic cancer. Hum Mol Genet 30: 485-499, 2021.

43. Xu WP, Cui YL, Chen LL, Ding K, Ding CH, Chen F, Zhang X and Xie WF: Deletion of Sox9 in the liver leads to hepatic cystogenesis in mice by transcriptionally downregulating Sec63. J Pathol 254: 57-69, 2021.
44. Schepers GE, Teasdale RD and Koopman P: Twenty pairs of sox: Extent, homology, and nomenclature of the mouse and human sox transcription factor gene families. Dev Cell 3: 167-170, 2002.
45. Tew SR and Hardingham TE: Regulation of SOX9 mRNA in human articular chondrocytes involving p38 MAPK activation and mRNA stabilization. J Biol Chem 281: 39471-39479, 2006.
46. Bao Z, Zhang N, Niu W, Mu M, Zhang X, Hu S and Niu C: Exosomal miR-155-5p derived from glioma stem-like cells promotes mesenchymal transition via targeting ACOT12. Cell Death Dis 13: 725, 2022.
47. Chen G, Wang D, Zhao X, Cao J, Zhao Y, Wang F, Bai J, Luo D and Li L: miR-155-5p modulates malignant behaviors of hepatocellular carcinoma by directly targeting CTHRC1 and indirectly regulating GSK-3β-involved Wnt/β-catenin signaling. Cancer Cell Int 17: 118, 2017.
48. Yang LW, Wu XJ, Liang Y, Ye GQ, Che YC, Wu XZ, Zhu XJ, Fan HL, Fan XP and Xu JF: miR-155 increases stemness and decitabine resistance in triple-negative breast cancer cells by inhibiting TSPAN5. Mol Carcinog 59: 447-461, 2020.
49. Wu HY, Liu K and Zhang JL: LINC00240/miR-155 axis regulates function of trophoblasts and M2 macrophage polarization via modulating oxidative stress-induced pyroptosis in preeclampsia. Mol Med 28: 119, 2022.